

The stellar mass – halo mass relation from galaxy clustering in VUDS: a high star formation efficiency at $z \approx 3$ *

A. Durkalec¹, O. Le Fèvre¹, S. de la Torre¹, A. Pollo^{19,20}, P. Cassata^{1,18}, B. Garilli³, V. Le Brun¹, B.C. Lemaux¹, D. Maccagni³, L. Pentericci⁴, L.A.M. Tasca¹, R. Thomas¹, E. Vanzella², G. Zamorani², E. Zucca², R. Amorín⁴, S. Bardelli², L.P. Cassarà³, M. Castellano⁴, A. Cimatti⁵, O. Cucciati^{5,2}, A. Fontana⁴, M. Giavalisco¹³, A. Grazian⁴, N. P. Hathi¹, O. Ilbert¹, S. Paltani⁹, B. Ribeiro¹, D. Schaerer^{10,8}, M. Scodeggio³, V. Sommariva^{5,4}, M. Talia⁵, L. Tresse¹, D. Vergani^{6,2}, P. Capak¹², S. Charlot⁷, T. Contini⁸, J.G. Cuby¹, J. Dunlop¹⁶, S. Fotopoulou⁹, A. Koekemoer¹⁷, C. López-Sanjuan¹¹, Y. Mellier⁷, J. Pforr¹, M. Salvato¹⁴, N. Scoville¹², Y. Taniguchi¹⁵, and P.W. Wang¹

¹ Aix Marseille Université, CNRS, LAM (Laboratoire d'Astrophysique de Marseille) UMR 7326, 13388, Marseille, France

² INAF-Osservatorio Astronomico di Bologna, via Ranzani,1, I-40127, Bologna, Italy

³ INAF-IASF, via Bassini 15, I-20133, Milano, Italy

⁴ INAF-Osservatorio Astronomico di Roma, via di Frascati 33, I-00040, Monte Porzio Catone, Italy

⁵ University of Bologna, Department of Physics and Astronomy (DIFA), V.le Berti Pichat, 6/2 - 40127, Bologna, Italy

⁶ INAF-IASF Bologna, via Gobetti 101, I-40129, Bologna, Italy

⁷ Institut d'Astrophysique de Paris, UMR7095 CNRS, Université Pierre et Marie Curie, 98b Boulevard Arago, Paris, France

⁸ Institut de Recherche en Astrophysique et Planétologie - IRAP, CNRS, Université de Toulouse, UPS-OMP, 14, avenue E. Belin, F31400 Toulouse, France

⁹ Department of Astronomy, University of Geneva, ch. d'cogia 16, CH-1290 Versoix, Switzerland

¹⁰ Geneva Observatory, University of Geneva, ch. des Maillettes 51, CH-1290 Versoix, Switzerland

¹¹ Centro de Estudios de Física del Cosmos de Aragón, Teruel, Spain

¹² Department of Astronomy, California Institute of Technology, 1200 E. California Blvd., MC 249-17, Pasadena, USA

¹³ Astronomy Department, University of Massachusetts, Amherst, MA 01003, USA

¹⁴ Max-Planck-Institut für Extraterrestrische Physik, Postfach 1312, D-85741, Garching bei München, Germany

¹⁵ Research Center for Space and Cosmic Evolution, Ehime University, Bunkyo-cho 2-5, Matsuyama 790-8577, Japan

¹⁶ SUPA, Institute for Astronomy, University of Edinburgh, Royal Observatory, Edinburgh, EH9 3HJ, United Kingdom

¹⁷ Space Telescope Science Institute, 3700 San Martin Drive, Baltimore, MD 21218, USA Instituto de Física y Astronomía, Facultad de Ciencias, Universidad de Valparaíso, Av. Gran Bretaña 1111, Casilla 5030, Valparaíso, Chile

¹⁸ Astronomical Observatory of the Jagiellonian University, Orla 171, 30-001 Cracow, Poland

¹⁹ National Centre for Nuclear Research, ul. Hoza 69, 00-681, Warszawa, Poland

Preprint online version: December 19, 2014

ABSTRACT

The relation between the galaxy stellar mass M_* and the dark matter halo mass M_h gives important information on the efficiency in forming stars and assembling stellar mass in galaxies. We present the stellar mass to halo mass ratio (SMHR) measurements at redshifts $2 < z < 5$, obtained from the VIMOS Ultra Deep Survey. We use halo occupation distribution (HOD) modelling of clustering measurements on ~ 3000 galaxies with spectroscopic redshifts to derive the dark matter halo mass M_h , and SED fitting over a large set of multi-wavelength data to derive the stellar mass M_* and compute the $SMHR = M_*/M_h$. We find that the SMHR ranges from 1% to 2.5% for galaxies with $M_* = 1.3 \times 10^9 M_\odot$ to $M_* = 7.4 \times 10^9 M_\odot$ in DM halos with $M_h = 1.3 \times 10^{11} M_\odot$ to $M_h = 3 \times 10^{11} M_\odot$. We derive the integrated star formation efficiency (ISFE) of these galaxies and find that the star formation efficiency is a moderate 6–9% for lower mass galaxies while it is relatively high at 16% for galaxies with the median stellar mass of the sample $\sim 7 \times 10^9 M_\odot$. The lower ISFE at lower masses may indicate that some efficient means of suppressing star formation is at work (like SNe feedback), while the high ISFE for the average galaxy at $z \sim 3$ is indicating that these galaxies are efficiently building-up their stellar mass at a key epoch in the mass assembly process. We further infer that the average mass galaxy at $z \sim 3$ will start experiencing star formation quenching within a few hundred millions years.

Key words. Cosmology: observations – large-scale structure of Universe – Galaxies: high-redshift – Galaxies: clustering

1. Introduction

Understanding processes regulating star formation and mass growth in galaxies along cosmic time remains a key issue of galaxy formation and evolution. In the Λ CDM model dark mat-

ter (DM) halos grow hierarchically, and galaxies are thought to form via dissipative collapse in the deep potential wells of these DM halos (e.g. White & Rees 1978, Fall & Efstathiou 1980). In this paradigm, cooling processes bring baryons in high density peaks of the matter density field (haloes), where the conditions for gas fragmentation trigger star formation (Bromm et al. 2009). Current models connecting star formation and stellar mass evolution on the one hand, and the for-

* Based on data obtained with the European Southern Observatory Very Large Telescope, Paranal, Chile, under Large Program 185.A-0791.

mation histories of DM halos on the other hand, are relying on simplifying assumptions and approximations and need to be further informed by observational data to reduce the uncertainties in the modelling process (e.g. Conroy & Wechsler 2009).

The efficiency of assembling baryons into stars is an important ingredient to understand galaxy formation but remains poorly constrained observationally. In recent years it has been proposed to derive this efficiency comparing DM halo mass with galaxy stellar mass. With the measurement of the characteristic mass of DM host haloes M_h now available from observational data and of stellar mass M_* derived from the analysis of the spectral energy distribution of galaxies, coupled to the knowledge of the cosmological density of baryons and DM, one can infer the conversion rate from baryons to stellar mass.

Two methods have been used so far to link M_* and M_h . Halo occupation models provide a description of how galaxies populate their host haloes using galaxy clustering statistics and local density profiles (e.g. Zehavi et al. 2005, Leauthaud et al. 2012). Alternatively, abundance matching associate galaxies to underlying dark matter structure and sub-structures assuming that the stellar masses or luminosities of the galaxies are tightly connected to the masses of dark matter halos (Conroy et al. 2009, Moster et al. 2013). The efficiency with which the galaxies converted baryons into stars is encoded in the relationship between M_* and M_h as a function of redshift, which provides a benchmark against which galaxy evolution models can be tested. Using observed stellar mass functions, abundance matching models have led to the derivation of the Stellar Mass – Halo Mass (SMHM) relation which gives for a given halo mass the Stellar Mass to Halo Mass ratio (SMHR), $SMHR = M_*/M_h$. Behroozi et al. (2010) find that the integrated star formation efficiency (ISFE) at a given halo mass peaks at 10-20% of available baryons for all redshifts from 0 to 4.

The shape of the SMHM is claimed not to evolve much from $z = 0$ to $z = 4$, although it may be evolving more significantly at $z > 4$ (Behroozi et al. 2013, Behroozi & Silk 2014). The SMHR is characterized by a maximum around $M_h = 10^{12} M_\odot$. The lower efficiency at masses below this value may indicate that supernova feedback might be sufficient to remove gas from the galaxy as the halo gravitational potential is lower (e.g. Silk 2003, Bertone et al. 2005, Béthermin et al. 2013). At higher masses, the decrease in star formation efficiency might be produced when cold streams are replaced by isotropic cooling (e.g. Dekel & Birnboim 2006, Faucher-Giguère et al. 2011) or by some high energy feedback process like that produced by AGNs.

While this picture is attractive from a theoretical modelling point of view, consistency with observational constraints need to be further improved. In this Letter we use the VIMOS Ultra Deep Survey (VUDS, Le Fèvre et al. 2014) to report on the first measurements of the SMHR derived from the observed clustering of galaxies at $2 < z < 5$. Using M_h derived from HOD modelling based on the two-point projected correlation function $w_p(r_p)$, and M_* obtained from SED fitting computed from ~ 3000 galaxies we estimate the SMHR for several galaxy samples, and compare it to SMHM models. The Letter is organized as follows: we summarize the VUDS data in Section 2, the M_h and M_* measurements are presented in Section 3, we derive the SMHR and the ISFE for several mass bins at $z \sim 3$ in Section 4, and we discuss our results in Section 5.

We use a flat Λ CDM cosmological model with $\Omega_m = 0.25$, and a Hubble constant $H_0 = 70 \text{ km s}^{-1} \text{ Mpc}$ to compute absolute magnitudes and masses.

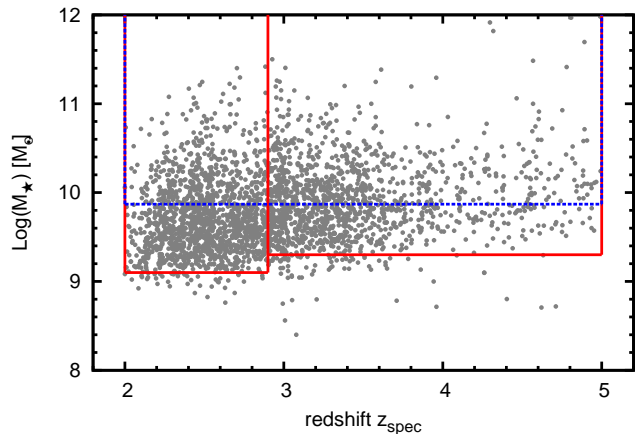


Fig. 1. Stellar mass distribution in VUDS. Red lines and horizontal lines indicate the limits in redshift and stellar mass applied to select low and high redshift samples. The dashed blue line indicate the mass cut at $M_* = 7.4 \times 10^9 M_\odot$ applied to define a high-mass sample.

2. The VUDS Data

The VIMOS Ultra Deep Survey (VUDS) is a spectroscopic survey of $\sim 10\,000$ galaxies performed with the VIMOS multi-object spectrograph at the European Southern Observatory Very Large Telescope Le Fèvre et al. (2003). Its main aim is to study early phases of galaxy formation and evolution at $2 < z < 6$. Details about the survey strategy, target selection, as well as data processing and redshift measurements are presented in Le Fèvre et al. (2014).

We use data in the redshift range $2 < z < 5$ from two independent fields, COSMOS and VVDS-02h, covering a total area 0.81 deg^2 , corresponding to a volume $\sim 3 \times 10^7 \text{ Mpc}^3$. The sample used here contains 3022 galaxies with reliable spectroscopic redshifts (spectroscopy reliability flags 2, 3, 4 and 9, see Le Fèvre et al. 2014) and with a stellar mass in the range $9 < \log(M_*) < 11 M_\odot$ as presented in Figure 1. The whole sample has been divided into two redshift ranges: $2 < z < 2.9$ with $\log M_*^{resh} = 9.1 M_\odot$ and $2.9 < z < 5.0$ for which $\log M_*^{resh} = 9.3 M_\odot$, where M_*^{resh} is the lower mass boundary of the sample resulting from the survey selection function (see below). Additionally, to estimate the SMHR for more massive galaxies we define a galaxy sub-sample in the range $2 < z < 5$ and with $\log M_* > 9.87 M_\odot$. This mass limit is the practical limit for which we can measure a galaxy correlation function signal accurately enough at each observed scale $0.3 < r_p < 17 h^{-1} \text{ Mpc}$, which is required in order to get the HOD fit to converge.

3. M_* and M_h measurements

The stellar masses in the VUDS survey are estimated by performing SED fitting on the multi-wavelength photometry using the 'Le Phare' code (Ilbert et al. 2006), as described in details by Ilbert et al. (2013) and references therein.

Halo masses M_h are measured from a two-step process. First, the projected two-point correlation function $w_p(r_p)$ is computed for all three sub-samples in Durkalec et al. (2014). The correlation function results are then interpreted in terms of a three-parameter halo occupation model (HOD) of the

Table 1. The stellar mass to halo mass ratio (SMHR), and the integrated star formation efficiency (ISFE) in the VUDS survey

Redshift range	z_{mean}	Stellar mass range	$\log M_{\star}^{resh}$	$\log M_h^{min}$	SMHR $\times 10^2$	ISFE $\times 10^2$
[2.0 – 2.9]	2.50	[9.10 – 11.40]	$9.10^{+0.15}_{-0.16}$	$11.12^{+0.33}_{-0.36}$	$0.95^{+0.50}_{-0.35}$	$6.16^{+3.23}_{-2.26}$
[2.9 – 5.0]	3.47	[9.30 – 11.40]	$9.30^{+0.17}_{-0.19}$	$11.18^{+0.56}_{-0.70}$	$1.32^{+0.98}_{-0.57}$	$8.52^{+6.32}_{-3.68}$
[2.0 – 5.0] ^a	3.00	[9.87 – 11.40]	$9.87^{+0.13}_{-0.15}$	$11.47^{+0.38}_{-0.43}$	$2.51^{+1.23}_{-0.89}$	$16.19^{+7.94}_{-5.74}$

^a high mass sample

form proposed by Zehavi et al. (2005) and motivated by Kravtsov et al. (2004), with the mean number of galaxies:

$$\langle N_g | M \rangle = \begin{cases} 1 + \left(\frac{M}{M_1}\right)^\alpha & \text{for } M > M_{min} \\ 0 & \text{otherwise,} \end{cases} \quad (1)$$

where M_{min} is the minimum mass needed for a halo to host one central galaxy, and M_1 is the mass of a halo having on average one satellite galaxy, while α is the power law slope of the satellite mean occupation function.

The correlation function measurements and model fitting procedures are described in Durkalec et al. (2014). By construction of the halo occupation function given in Eq. 1, the parameter M_{min} is the halo mass associated to galaxies with a stellar mass defined as the stellar mass threshold in the SHM relation (Zheng et al. 2005; Zehavi et al. 2005). We therefore quote the lowest mass of the sample considered as M_{\star}^{resh} , as imposed by the survey limiting magnitude. The errors associated to this lower limit have been computed as the average of the errors on M_{\star} from the SED fitting for each redshift and mass sub-sample separately.

4. The stellar mass – halo mass relation at $z \sim 3$

Our results are presented in Table 1 and in the left panel of Figure 2. We find that for the low redshift sample $z \sim 2.5$ the stellar mass for halos of mass $\log M_h^{min} = 11.12 \pm 0.33 M_{\odot}$ is $\log M_{\star}^{resh} = 9.1 M_{\odot}$, while at $z \sim 3.5$ the halo mass reaches $\log M_h^{min} = 11.18 \pm 0.56 M_{\odot}$ for a stellar mass $\log M_{\star}^{resh} = 9.3 M_{\odot}$.

From these measurements we find that $\log(M_{\star}/M_h)$ is ranging from -2.02 ± 0.18 for the low mass sample up to -1.6 ± 0.17 for the most massive sample, at a redshift $z \sim 3$. As shown in Figure 2 these results are compared to various measurements at low and intermediate redshift $z < 1$, obtained using different methods, including satellite kinematics (Conroy et al. 2007, More et al. 2011), weak lensing (Mandelbaum et al. 2006), galaxy clustering (Foucaud et al. 2010, Hartley et al. 2013), as well as abundance matching (Moster et al. 2013). Our measurements are in excellent agreement with models derived from abundance matching at a redshift $z = 3$ (Moster et al. 2013).

5. Discussion and conclusion

Our SMHR measurements are among the first performed at $z \sim 3$ from a clustering and HOD analysis, as made possible from the large VUDS spectroscopic redshift survey. We find that the SMHR is 1% to 2.5% for galaxies with intermediate stellar masses (at $z \sim 3$) ranging from $\sim 10^9 M_{\odot}$ to $\sim 7 \times 10^9 M_{\odot}$.

Following Conroy & Wechsler (2009) we compute the integrated star formation efficiency (ISFE) $\eta = M_{\star}/M_h/f_b$ with f_b

the universal baryon fraction $f_b = \Omega_b/\Omega_m = 0.155$ (Planck collaboration 2014). Results are reported in Table 1. We find that the ISFE range from $6.2^{+3.2}_{-2.3}\%$ to $16.2^{+7.9}_{-5.7}\%$ for galaxies with M_{\star} from $M_{\star}^{resh} = 1.3 \times 10^9 M_{\odot}$ to $M_{\star}^{resh} = 7.4 \times 10^9 M_{\odot}$. The ISFE at $z \sim 3$ therefore increases with M_{\star} over this mass range. The star formation efficiency of $\sim 16\%$ in a halo with $M_h = 3 \times 10^{11} M_{\odot}$ is quite close to a maximum of $\sim 20\%$ occurring at $10^{12} M_{\odot}$ in SMHM models Behroozi et al. (2010) (see also Moster et al. 2013).

We use a simple mass growth model to derive the time scale for which our most massive galaxy sample would reach the maximum predicted in the SMHM relation from Behroozi et al. (2010). In this model the mass growth of DM haloes is described by a mean accretion rate $\langle \dot{M}_H \rangle_{mean}$ taken from Fakhouri et al. (2010), while galaxies grow in M_{\star} via star formation using the median SFR for our sample (Tasca et al. 2014a), as well as through mergers with a constant accretion in stars of $\sim 1 M_{\odot}/yr$ (Tasca et al. 2014b). We compute the halo and stellar mass values every $\delta t = 5$ Myr to account for the halo accretion rate and SFR changing with redshift and mass. In the right panel of Figure 2 we represent the expected time evolution in M_{\star}/M_h versus M_{\star} for a galaxy starting at $z \sim 3$ following this ‘toy model’. We find that the SMHM relation would reach a maximum $\log(M_{\star}/M_h) \simeq -1.25$ about 360 Myr after the observed epoch (i.e. at $z \sim 2.6$) and that at this time halo and stellar masses will be $M_h^{min} = 10^{11.6} M_{\odot}$ and $M_{\star}^{resh} = 2 \times 10^{10} M_{\odot}$ respectively.

According to the model proposed by Moster et al. (2013) the SMHM relation should turn over after reaching a maximum, with the slope of the relation maintaining the same absolute value but reversing sign (see Figure 2). Since dark matter halos grow in time (e.g. Fakhouri et al. 2010) the growth in stellar mass must drop dramatically over a sustained period of time in order to follow a change in M_{\star}/M_h by roughly an order of magnitude in the SMHM, or, alternatively, the dark matter accretion rate $\langle \dot{M}_H \rangle$ must rise precipitously, or a combination of the two. There are no indications e.g. in N-body simulations which support a dramatic sustained rise in $\langle \dot{M}_H \rangle$. On the other hand the stellar mass computed at the maximum of the SMHM relation is $M_{\star} \sim 2 \times 10^{10} M_{\odot}$, comparable to the ‘quenching mass’ as discussed in Bundy et al. (2006) and is massive enough at $z \sim 2.6$ that mass-related quenching may be dominant (Peng et al. 2010). In this picture, on average, the massive galaxy population in VUDS with $M_{\star}^{min} \sim 0.5 - 1 \times 10^{10} M_{\odot}$ observed at $z \sim 3$ will experience star formation quenching within a few hundred million years. Assuming that the SFR will successfully drop and will reach zero when the halo mass grows by 0.5 dex (the approximate width the peak of the SMHM relation), we compute that the star formation will then be quenched within ~ 2 Gyr (by $z \sim 1.5$). After that time the stellar mass

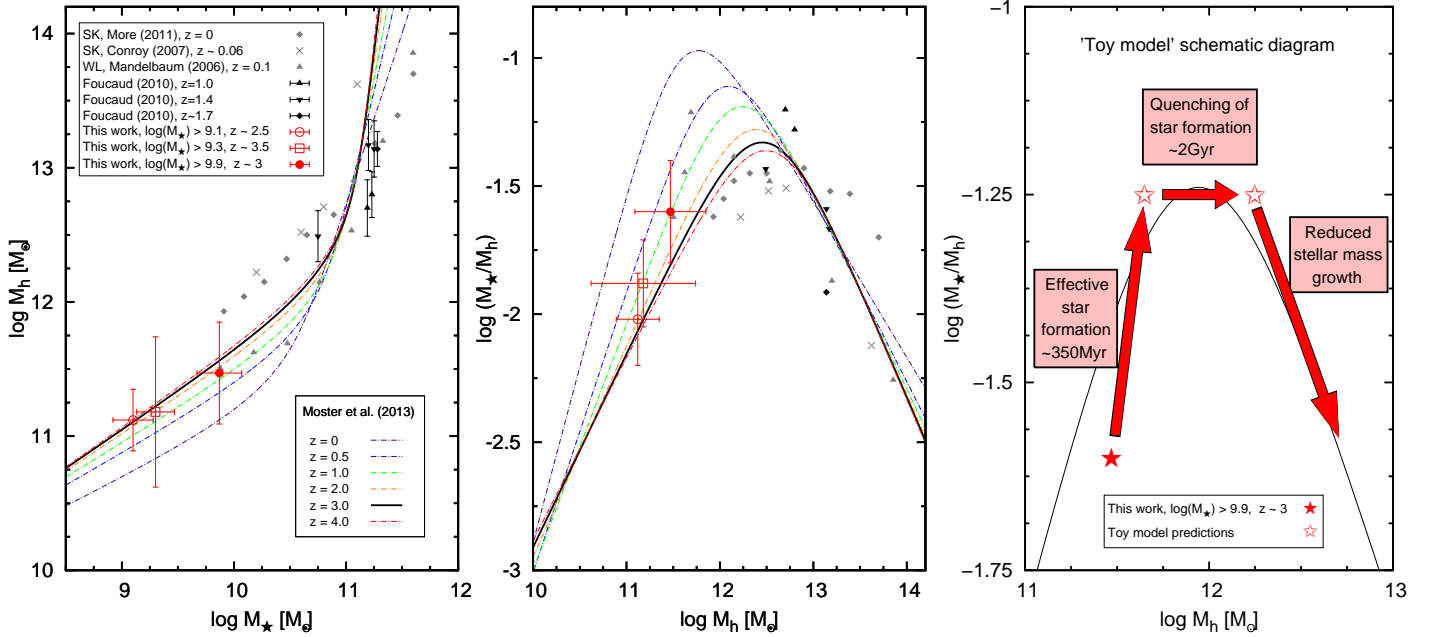


Fig. 2. *Left:* The relation between the stellar mass M_* and the halo mass M_h in VUDS for different M_* and redshifts (red symbols). M_* is derived from SED fitting of the multi-wavelength photometric data using known spectroscopic redshifts; error bars in M_* indicate expected uncertainties of the SED fitting method. M_h is obtained from HOD modelling of the two-point correlation function in different redshift and mass ranges. The VUDS data is compared to low and intermediate redshift measurements from satellite kinematics (Conroy et al. 2007; More et al. 2011) weak lensing (Mandelbaum et al. 2006), galaxy clustering (Foucaud et al. 2010). The lines represents model predictions derived from abundance matching at various redshift (Moster et al. 2013). *Center:* The stellar mass M_* over halo mass M_h ratio vs. halo mass at $z = 3$ in the VUDS survey. The colour scheme is the same as for the left panel. *Right:* Evolution of the M_*/M_h ratio with time predicted from stellar and halo mass accretion histories for the most massive galaxy population observed at $z \sim 3$, using the ‘toy model’ described in the text.

would grow only slowly e.g. through mergers and/or lower levels of star formation in order for galaxy populations to follow the SMHM relation.

In conclusion, the SMHM is a simple yet efficient tool to probe star formation efficiency at the epoch of rapid stellar mass assembly provided one obtains robust measurements on both M_* and M_h ; this is now possible with VUDS at $z \sim 3$, complementing more indirect estimates using e.g. abundance matching. A more extensive exploration of the efficiency of star formation over a larger range of halo masses is becoming possible with new surveys, and it would be interesting to probe higher masses than done in this paper to evaluate the halo mass corresponding to the highest star formation efficiency. Extending such measurements to higher redshifts will require the power of new facilities like PFS-Sumire, JWST or ELTs.

Acknowledgements. We thank Jean Coupon and Carlo Schimid for interesting discussions. This work is supported by the European Research Council Advanced Grant ERC-2010-AdG-268107-EARLY, and by INAF Grants PRIN 2010&2012 and PICS 2013. AC, OC, MT and VS acknowledge the grant MIUR PRIN 2010–2011. This work is supported by the OCEVU Labex (ANR-11-LABX-0060) and the A³MIDEX project (ANR-11-IDEX-0001-02). AP is supported by grant UMO-2012/07/B/ST9/04425 and the Polish-Swiss Astro Project. Research conducted within the scope of the HECOLS International Associated Laboratory, supported in part by the Polish NCN grant DEC-2013/08/M/ST9/00664. This work is based on data products made available at the CESAM data center, Laboratoire d’Astrophysique de Marseille, France.

References

Behroozi, P. S., Conroy, C., & Wechsler, R. H. 2010, *ApJ*, 717, 379
 Behroozi, P. S. & Silk, J. 2014, *ArXiv e-prints*

Behroozi, P. S., Wechsler, R. H., & Conroy, C. 2013, *ApJ*, 762, L31
 Bertone, S., Stoehr, F., & White, S. D. M. 2005, *MNRAS*, 359, 1201
 Béthermin, M., Wang, L., Doré, O., et al. 2013, *A&A*, 557, A66
 Bromm, V., Yoshida, N., Hernquist, L., & McKee, C. F. 2009, *Nature*, 459, 49
 Bundy, K., Ellis, R. S., Conselice, C. J., et al. 2006, *ApJ*, 651, 120
 Conroy, C., Gunn, J. E., & White, M. 2009, *ApJ*, 699, 486
 Conroy, C., Prada, F., Newman, J. A., et al. 2007, *ApJ*, 654, 153
 Conroy, C. & Wechsler, R. H. 2009, *ApJ*, 696, 620
 Dekel, A. & Birnboim, Y. 2006, *MNRAS*, 368, 2
 Durkalec, A., Le Fèvre, O., Pollo, A., et al. 2014, *ArXiv e-prints*
 Fakhouri, O., Ma, C.-P., & Boylan-Kolchin, M. 2010, *MNRAS*, 406, 2267
 Fall, S. M. & Efstathiou, G. 1980, *MNRAS*, 193, 189
 Faucher-Giguère, C.-A., Kereš, D., & Ma, C.-P. 2011, *MNRAS*, 417, 2982
 Foucaud, S., Conselice, C. J., Hartley, W. G., et al. 2010, *MNRAS*, 406, 147
 Hartley, W. G., Almaini, O., Mortlock, A., et al. 2013, *MNRAS*, 431, 3045
 Ilbert, O., Arnouts, S., McCracken, H. J., et al. 2006, *A&A*, 457, 841
 Ilbert, O., McCracken, H. J., Le Fèvre, O., et al. 2013, *A&A*, 556, A55
 Kravtsov, A. V., Berlind, A. A., Wechsler, R. H., et al. 2004, *ApJ*, 609, 35
 Le Fèvre, O., Saisse, M., Mancini, D., et al. 2003, in *SPIE Conference Series*, Vol. 4841, Instrument Design and Performance for Optical/Infrared Ground-based Telescopes, ed. M. Iye & A. F. M. Moorwood, 1670–1681
 Le Fèvre, O., Tasca, L. A. M., Cassata, P., et al. 2014, *ArXiv e-prints*
 Leauthaud, A., Tinker, J., Bundy, K., et al. 2012, *ApJ*, 744, 159
 Mandelbaum, R., Seljak, U., Kauffmann, G., Hirata, C. M., & Brinkmann, J. 2006, *MNRAS*, 368, 715
 More, S., van den Bosch, F. C., Cacciato, M., et al. 2011, *MNRAS*, 410, 210
 Moster, B. P., Naab, T., & White, S. D. M. 2013, *MNRAS*, 428, 3121
 Peng, Y.-j., Lilly, S. J., Kovač, K., et al. 2010, *ApJ*, 721, 193
 Silk, J. 2003, *MNRAS*, 343, 249
 Tasca, L. A. M., Le Fèvre, O., Hathi, N. P., et al. 2014a, *ArXiv e-prints*
 Tasca, L. A. M., Le Fèvre, O., López-Sanjuan, C., et al. 2014b, *A&A*, 565, A10
 White, S. D. M. & Rees, M. J. 1978, *MNRAS*, 183, 341
 Zehavi, I., Zheng, Z., Weinberg, D. H., et al. 2005, *ApJ*, 630, 1
 Zheng, Z., Berlind, A. A., Weinberg, D. H., et al. 2005, *ApJ*, 633, 791